Check for updates

Batteries & Supercaps

Reviews
doi.org/10.1002/batt.202000283

Chemistry Europe
European Chemical Societies Publishing

Special Collection

Application of In Situ Raman and Fourier Transform Infrared Spectroelectrochemical Methods on the Electrode-Electrolyte Interface for Lithium–Oxygen Batteries

Chunguang Chen,[a, b] Mengyuan Song,[b] Lingzhu Lu,[a] Lijuan Yue,[a] Tao Huang,[c] and Aishui Yu*[b]

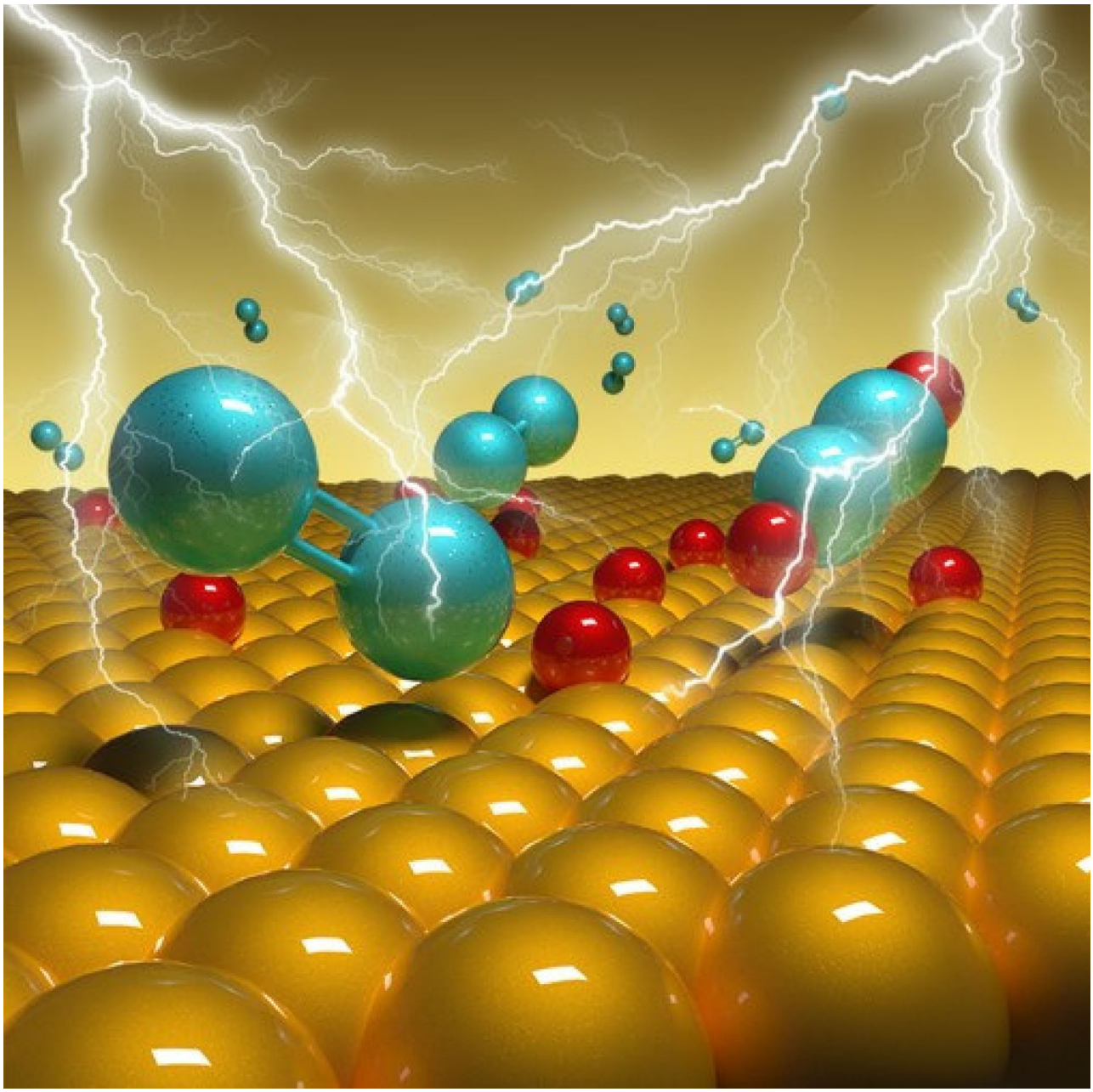

© 2021 Wiley-VCH GmbH

25666223, 2021, 6, Downloaded from https://chemistry-europe.onlinelibrary.wiley.com/doi/10.1002/batt.202000283 by University of Ulsan, Wiley Online Library on [11/11/2025]. See the Terms and Conditions (https://onlinelibrary.wiley.com/terms-and-conditions) on Wiley Online Library for rules of use; OA articles are governed by the applicable Creative Commons License

The development of rechargeable lithium–oxygen ($Li–O_2$) batteries with high specific energy is essential to satisfy increasing energy consumption. It is critical to understand the dynamic process and detailed pathways during cell operation, which will allow us to control the reaction, suppress the formation of byproducts, and optimize battery performance. In situ vibrational spectroelectrochemical techniques, including in situ Raman spectroscopy and in situ Fourier Transform Infrared (FTIR) spectroscopy, are powerful analytical methods for the purposes of battery studies and are reviewed in this article. The two in situ techniques can acquire real-time information of adsorbed species on the interface of the electrode, and reveal the reaction mechanism on the interface of the electrode/electrolyte in depth. In situ Raman technique mainly monitors intermediate species and products in $Li–O_2$ batteries. The applications of surface-enhanced Raman spectroscopy (SERS) for $Li–O_2$ batteries are described in detail in the review. For the in situ FTIR technique, two commonly used in situ methods are introduced in $Li–O_2$ batteries, namely, subtractive normalized Fourier transform infrared spectroscopy (SNIFTIRS) and attenuated total reflection surface enhanced infrared absorption spectroscopy (ATR-SEIRAS). The reaction mechanism and failure mechanism of the cell are discussed by using the in situ FTIR technique.

1. Introduction

$Li–O_2$ batteries have been focus of attention over the past few decades because of the high theoretical energy density,[1] which could satisfy the increasing needs of electric vehicles and portable electronic devices. Despite its potential, $Li–O_2$ batteries have not yet been put into practical use because some fundamental problems remain to be solved, including understanding the battery performance and designing practical cell architectures.

For an ideal $Li–O_2$ battery, Li^+ reacts with gaseous O_2 at a porous cathode electrode to form lithium peroxide during discharge, and the process is reversed upon charge.[2] Owing to the complex solid/liquid/gas three-phase reaction interface, the reaction routes, intermediates and reaction products are still unclear in $Li–O_2$ batteries. These factors significantly affect the cell performance, such as cell capacity, power density and cyclability. In order to understand the battery behavior, the influence of electrode materials, and the composition of electrolyte as well as the intermediate products need to be investigated. To date, different techniques, especially real-time monitoring in situ methods, have been used to characterize such information, including X-ray diffraction (XRD), X-ray photoelectron spectroscopy (XPS), Raman spectroscopy, FTIR spectroscopy, and sum-frequency generation (SFG) spectroscopy.[3] In this review, we highlight the applications of two in situ vibrational spectroelectrochemical techniques (Raman and FTIR) for $Li–O_2$ batteries, which can probe the structures at an atomic scale.

Raman spectroscopy is based on a change in the polarizability of vibrational materials, which resulting in the Raman effect.[4] The vibrational transitions in the homopolar bindings (such as O–O) can be obtained by Raman spectra, while it is no IR active. As a result, most applications of Raman spectroscopy in $Li–O_2$ batteries mainly focus on determining the oxygenated species, such as intermediate species (O_2^-, LiO_2) and Li_2O_2.[1b,5] The in situ SERS technique, offers an effective method to identify low concentration adsorbed species on the surface of an electrode, which can provide more evidence to support the presence of superoxide species and Li_2O_2 products in $Li–O_2$ batteries. FTIR spectroscopy, is based on a change of the vibrational modes in the electric dipole moment.[6] Therefore, FTIR spectroscopy can offer complementary information which is hardly obtained from Raman spectroscopy. Combined with the electrochemical methods, FTIR spectroscopy has been proven to be a powerful experimental technique to acquire molecular information and solution species involved in electrochemical reactions.[7] Two commonly used in situ FTIR methods, SNIFTIRS and ATR-SEIRAS are described. Intermediate products, reaction mechanism, decomposition of electrolytes, and the key factors affecting them are summarized. Based on the application of in situ Raman and FTIR in $Li–O_2$ batteries, real-time monitoring of liquid/solid interface processes is essential for understanding the reaction mechanism and failure mechanism in $Li–O_2$ batteries, and is also of great significance for the development of a suitable electrode/electrolyte combination.

2. In Situ Raman Techniques

Raman spectroscopy is an important vibrational spectroscopic technique, which utilizes the inelastic scattering of monochromatic light to detect molecular vibrations and crystal structures.[4] Compared with optical processes like absorption and fluorescence, Raman scattering is an extremely weak process (≈ 1 in 10^7 photons), leading to low sensitivity for

[a] Dr. C. Chen, L. Lu, L. Yue
Department of Chemistry, College of Science
University of Shanghai for Science and Technology
Shanghai 200093, China
E-mail: cgchen19@usst.edu.cn
[b] Dr. C. Chen, M. Song, Prof. A. Yu
Department of Chemistry,
Shanghai Key Laboratory of Molecular Catalysis and Innovative Materials
Institution of New Energy,
Collaborative Innovation Center of Chemistry for Energy Materials
Fudan University
Shanghai 200438, China
E-mail: asyu@fudan.edu.cn
[c] Dr. T. Huang
Laboratory of Advanced Materials
Fudan University
Shanghai 200438, China
E-mail: huangt@fudan.edu.cn

Special Collection An invited contribution to a joint Special Collection between ChemElectroChem and Batteries & Supercaps dedicated to research Beyond Lithium-Ion Batteries

© 2021 Wiley-VCH GmbH

Raman spectroscopy. By designing rough metal (Au, Ag or Cu) surfaces[8] on the substrate surface, the Raman signal is significantly enhanced (as high as 10^4 times). This technique is called surface-enhanced Raman spectroscopy (SERS).[9] With the SERS mode, detection sensitivity can even down to a signal molecule on the surface.[10] For in situ application of Li–O_2 batteries, we mainly focus on the SERS mode.

In situ SERS technique has been deployed to detect reaction intermediates or products (such as O_2^-, LiO_2 and Li_2O_2) on the cathode surfaces, offering an understanding of the reaction mechanism for the Li–O_2 batteries.[11] In the early study, Bruce and Peng et al.[12] investigated the reaction products at different charge and discharge potentials with acetonitrile (CH_3CN) electrolyte in Li–O_2 batteries based on the SERS mode. As shown in Figure 1, it revealed that O_2 is first reduced to O_2^- (ν_{O-O} 1109 cm^{-1}) or LiO_2 (O–O stretch of LiO_2 at 1137 cm^{-1}) intermediates in the absence or presence of Li^+ during the discharge process, and the LiO_2 intermediate is eventually converted into Li_2O_2 (O–O stretch of Li_2O_2 at 808 cm^{-1}). On charging, Li_2O_2 is decomposed directly to O_2 with

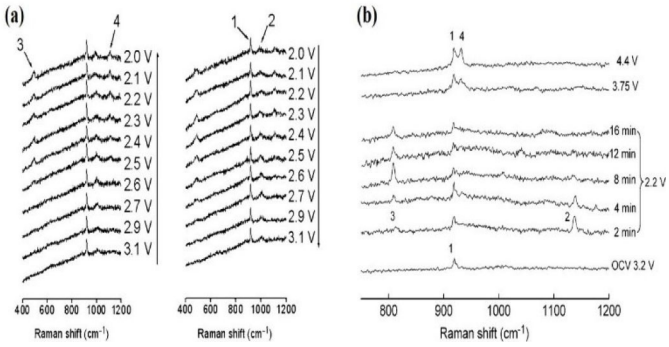

Figure 1. In situ SERS spectra obtained from a roughened Au electrode in O_2 saturated state a) 0.1 M nBu_4NClO_4–CH_3CN. Peak assignments are as follows: 1 and 2 corresponded to CH_3CN and nBu_4N^+, respectively, and 3 and 4 correspond to the Au–O stretch adsorbed O_2^- and O–O stretch of adsorbed O_2^-, respectively. b) 0.1 M $LiClO_4$–CH_3CN. Peak assignments are as follows: 1 and 4 correspond to CH_3CN and ClO_4^-, respectively, and 2 and 4 correspond to the O–O stretch of LiO_2 and O–O stretch of Li_2O_2, respectively. Reproduced from Ref. [12] with permission. Copyright (2011) Wiley-VCH.

Chunguang Chen received her Ph.D. in Physical Chemistry from Fudan University in 2019, and later worked as a lecturer fellow at Department of Chemistry, College of Science, University of Shanghai for Science and Technology. Her major research interests focus on interface research using various spectral methods and the energy active materials in lithium–air batteries.

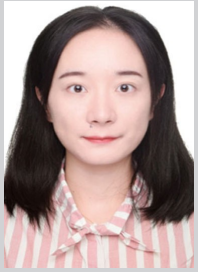

Mengyuan Song received her bachelor's degree from Qingdao University in 2019. She is currently pursuing her Ph.D. degree in the Research Group of Professor Aishui Yu at Fudan University. Her main research interests focus on the optimization of electrolyte and the interface research of lithium–air batteries.

Lingzhu Lu is currently a Master student majoring in Physical Chemistry at the University of Shanghai for Science and Technology in 2019. Her major research interests focus on the energy active materials and their application in lithium–air batteries.

Lijuan Yue is currently a Master student majoring in Physical Chemistry at the University of Shanghai for Science and Technology in 2020. Her major research interests focus on the energy active materials and their application in lithium–air batteries.

Tao Huang obtained her Ph.D. in Physical Chemistry from Xiamen University in 2007 and later worked as a postdoctoral fellow at Department of Chemistry, Fudan University. She is a Senior Engineer of Laboratory of Advanced Materials at Fudan University. Her research interests include lithium-ion batteries and lithium–air batteries.

Prof. Aishui Yu got his Ph.D. from Fudan University in 1993. He began his academic career as a lecturer at Fudan University in 1993. In 1995–1997, he was a Foreign Scholar at Iwate University in Japan. In 1995–1997, he worked at the Institute of Materials Research and Engineering in Singapore. After postdoctoral research in Department of Chemistry in University of Oklahoma (1997–1999), he was a Senior Scientist in Excellatron Solid State LLC in USA (2000–2006). He joined Fudan University as a Professor in 2006. His research interests include lithium-ion batteries, lithium–air batteries, solid state lithium batteries and lithium–sulfur batteries.

© 2021 Wiley-VCH GmbH

25666223, 2021, 6, Downloaded from https://chemistry-europe.onlinelibrary.wiley.com/doi/10.1002/batt.202000283 by University of Ulsan, Wiley Online Library on [11/11/2025]. See the Terms and Conditions (https://onlinelibrary.wiley.com/terms-and-conditions) on Wiley Online Library for rules of use; OA articles are governed by the applicable Creative Commons License

a one-step reaction and no production of LiO_2 intermediate species was detected.

Subsequently, DMSO, a more practical solvent in Li–O_2 batteries, is applied as the basic electrolyte to establish a reaction mechanism in the cell. Peng et al.[1b] provided convincing evidence of Li_2O_2 formation and evolution in DMSO-based electrolytes based on in situ Raman technology. Ye' s group[5a] systematically evaluated the ORR and OER processes of DMSO-based electrolytes on a sputtered Au electrode with the in situ SERS method. They concluded that the types of cations (TBA^+ and Li^+) in DMSO-based electrolytes have a great influence on the reaction mechanism of the cell. As shown in Figure 2a and 2c, during the ORR (red) process in the Li^+-free DMSO electrolyte (TBA^+ cation), two Raman peaks appeared around 490 and 1105 cm^{-1} at 2.6 V, which can be assigned to Au–O stretching and O–O stretching modes, respectively, for O_2^- adsorbed on a gold surface.[12–13] The intensities of the two peaks increased with the cathodic current flow and then decreased with the anodic current flow, finally disappearing around 3.6 V. The result indicated that the ORR and OER processes involve a one-electron transfer on the gold electrode surface, namely, $O_2 + e^- \rightleftharpoons O_2$. In the Li^+-containing DMSO electrolyte, both the electrochemical curve and SERS spectra were significantly different (Figure 2b and 2d). During the ORR process, two reduction peaks were observed and a new Raman peak appeared around 788 cm^{-1} in the second cathodic peak region, which could be assigned to the O–O stretching mode of Li_2O_2. The new Raman peak completely disappeared around 3.7 V when the cathodic current flowed. No any new Raman peaks of other oxygen species were detected, such as the LiO_2 intermediate, which had been detected using in situ UV-Vis characterization in this article. They explained that LiO_2 is generated in the bulk solution, making it difficult to be observed using the SERS measurement. Subsequently, it was further reduced to peroxide Li_2O_2. They concluded that O_2 was finally reduced to Li_2O_2 with a two-electron transfer in the Li^+-containing DMSO electrolyte, namely, $O_2 + 2Li^+ + 2e^- \rightleftharpoons Li_2O_2$. It is important to note that the signals of the products with Raman active, which are adsorbed on the electrode surface and not generated in the solution, can be monitored using the SERS technique. Therefore, more methods to characterize how the products behave on the electrode surface and in the solution are necessary.

In fact, some arguments are still present for the reaction mechanism in DMSO-based electrolytes. Taylor and co-workers[14] provided a different conclusion in DMSO-based electrolytes with a gold electrode using the in situ SERS technique. They found the LiO_2 Raman peak (~1140 cm^{-1}) and did not observe the Li_2O_2 Raman peak (~790 cm^{-1}) during the 1st discharge. During the charge process, the peak intensity of LiO_2 features at 1140 cm^{-1} decreased. They concluded that LiO_2 is mainly a final product and it can be reversibly formed and evolved upon cycling. This was not consistent with the previous work,[15] which focused on the generation and evolution of Li_2O_2. Obviously, the reaction mechanism is still ambiguous and more experiments as well as discussions are necessary in the future to clarify these issues.

In situ SERS has been applied to study the solvent effect for the ORR mechanism in Li–O_2 batteries. Using time-resolved SERS spectra with a roughened gold electrode, Johnson and Bruce[13a] investigated the intermediate species and products during the ORR process in the following four solvents, 1-methylimidazole (Me–Im), DMSO, dimethoxyethane (DME), and CH_3CN (Figure 3). A new peak was detected at ~1100 cm^{-1} when cathodic potential flowed to red point both in the Me–Im and DMSO electrolyte systems, which corresponded to the adsorbed O_2^-.[5a,16] The peak disappeared as the polarization time and cathodic overpotential increased. A new peak at ~790 cm^{-1} appeared, which was assigned to Li_2O_2.[1b] However, different features were obtained in the DME and CH_3CN

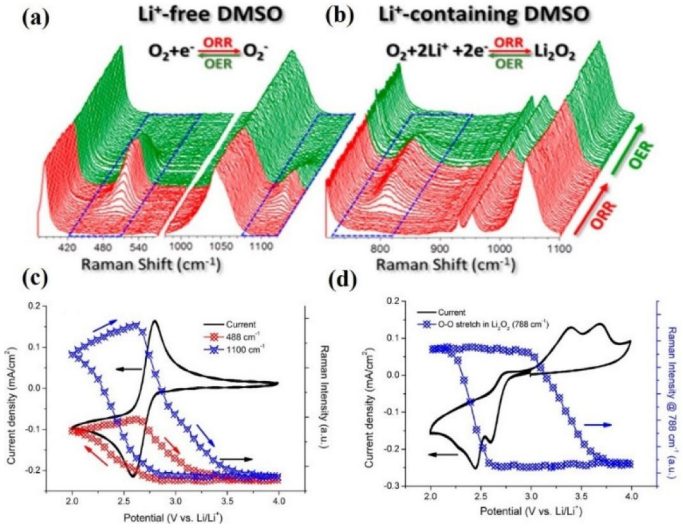

Figure 2. In situ SERS spectra (a and b) and the potential dependence of the Raman peak intensity (c and d) on the gold electrode surface in O_2 saturated atmosphere. The electrolyte systems are 0.1 M $TBAClO_4$–DMSO (a and c) and 0.1 M $LiClO_4$–DMSO (b and d). Reproduced from Ref. [5a] with permission. Copyright (2015) American Chemical Society.

© 2021 Wiley-VCH GmbH

25666223, 2021, 6, Downloaded from https://chemistry-europe.onlinelibrary.wiley.com/doi/10.1002/batt.202000283 by University of Ulsan, Wiley Online Library on [11/11/2025]. See the Terms and Conditions (https://onlinelibrary.wiley.com/terms-and-conditions) on Wiley Online Library for rules of use; OA articles are governed by the applicable Creative Commons License

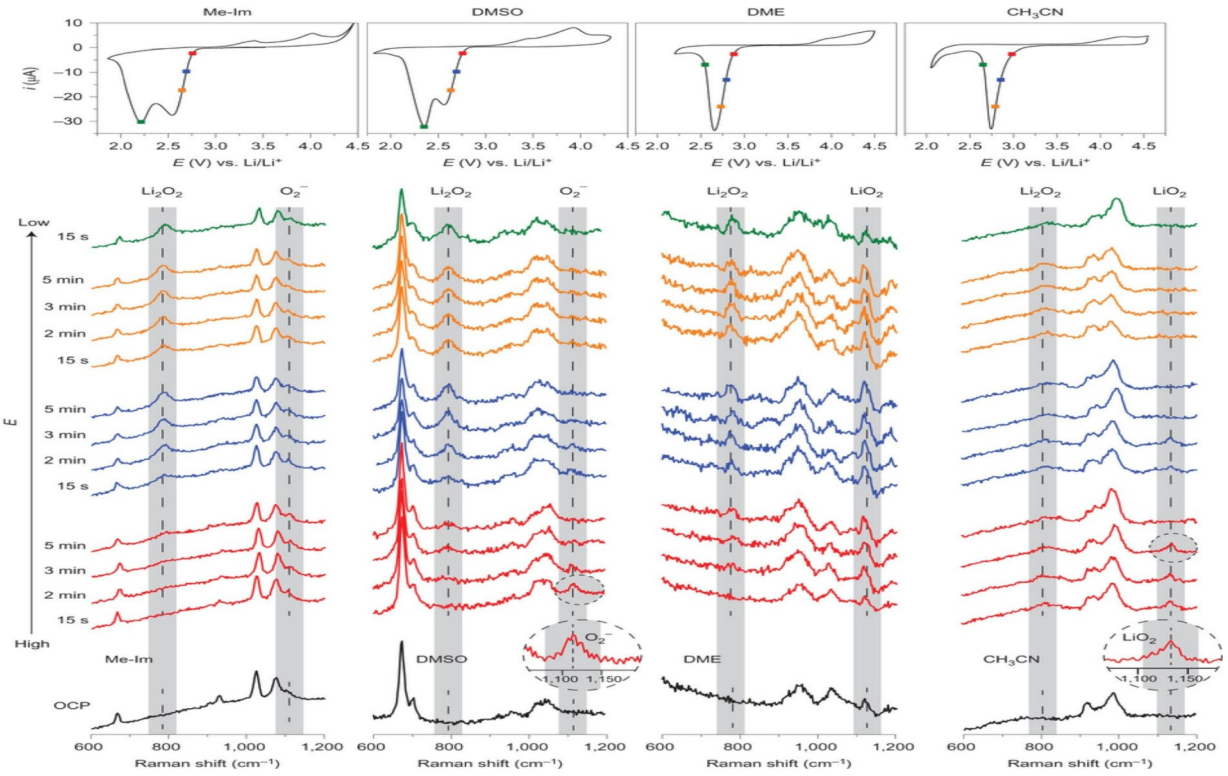

Figure 3. SERS spectra demonstrating that at low cathodic overpotentials O_2^- and LiO_2 species are observed on the electrode surface at short times in high- and low-DN solvents, respectively, to be replaced by Li_2O_2 over time. At low cathodic overpotentials Li_2O_2 is apparent from short times. Spectra collected at a gold electrode during O_2 reduction in the presence of 0.1 M $LiClO_4$ in various aprotic solvents, recorded at different times at various constant potentials indicated by the matching colored markers in the CVs above each stack of spectra. Vertical dotted lines with grey shading show positions of O_2^-, LiO_2 and Li_2O_2. Insets: expanded areas of spectral regions outlined by the dashed circles. Spectra at the bottom were collected at the open circuit potential. Reproduced from Ref. [13a] with permission. Copyright (2014) Nature Publishing Group.

electrolyte systems. A peak appeared at ~1132 cm^{-1} in the low overpotential region, which was assigned to adsorbed LiO_2.[16] At the high overpotential region, the peak disappeared and an Li_2O_2 (~790 cm^{-1}) peak occurred. Based on the SERS results, the authors suggested that a solution-based pathway (O_2^-) occurs during the ORR process with a high donor number (Me–Im or DMSO), while a surface-based pathway occurs with a low donor number (DME or CH_3CN).

The feature intensities of Li_2O_2 and the exact vibrational frequency of superoxide were found to be dependent upon its morphology and its environments, respectively, using Raman spectroscopy. Recent literatures have suggested that there are two main Li_2O_2 morphologies, the amorphous and the toroidal morphology.[17] According to the modeling study, amorphous species would be slightly more undercoordinated than the toroidal species and would have more lithium vacancy and hole polaron defects, which may lead to shorter O–O bonds.[18] That is to say, amorphous Li_2O_2 could be more easily detected by Raman spectroscopy and may have a higher O–O vibrational frequency than Li_2O_2 with toroidal morphology. For the superoxide (O_2^-/LiO_2) species, the environment (including factors such as cation, solvent, temperature etc.) affect the O–O bond. Rittner[19] and Andrews[20] reported that a more polarizable cation will have a higher O–O vibrational frequency because of a strong ability to attract electrons from the O–O anti-bond orbital. For example, the vibrational frequency of LiO_2 is 1097 cm^{-1}, while that of KO_2 is 1108 cm^{-1} in an argon atmosphere at 4 K.[20] At room temperature, the vibrational frequency of KO_2 shifts to ≈1145 cm^{-1}.[21] The vibrational frequency of O_2^- is ≈1110 cm^{-1} in two ionic liquids,[22] while a superoxide complex in DMSO is ≈1160 cm^{-1}.[23] Obviously, the influence of Li_2O_2 morphology and the environment surrounding the superoxide ion in a Raman test will interfere with our judgment of the species produced. Despite the challenges, significant evidences have confirmed that Li_2O_2 can be identified by Raman spectroscopy and the exact vibrational frequency of superoxide requires further studies.

It is worth noting that most of the SERS modes are only carried out on precious metal (Au or Ag) surfaces, which have limited capacity for investigating the electrochemical interfaces of Li–O_2 batteries. Precious metal and other materials (such as carbon et al.) are important catalysts in the real Li–O_2 batteries. In order to overcome this obstacle, the shell isolated nanoparticles for enhanced Raman spectroscopy (SHINERS) method is applied. Hardwick et al.[24] detected the oxygen reduction species on four different catalysts (glassy carbon, gold, palladium and platinum) in the presence of Li^+ using the SHINERS mode. They found that the peak positions of the O–O stretching mode of the O_2^- species adsorbed on different electrode surfaces were different. In addition, using the SHINERS mode, this study also proved that both the electrode surface and solvent are key factors in influencing the ORR

© 2021 Wiley-VCH GmbH

25666223, 2021, 6, Downloaded from https://chemistry-europe.onlinelibrary.wiley.com/doi/10.1002/batt.202000283 by University of Ulsan, Wiley Online Library on [11/11/2025]. See the Terms and Conditions (https://onlinelibrary.wiley.com/terms-and-conditions) on Wiley Online Library for rules of use; OA articles are governed by the applicable Creative Commons License

mechanism, which is critical in optimizing electrode/electrolyte interfaces that can effectively minimize side reactions for Li–O_2 batteries.

3. In Situ FTIR Technique

FTIR spectroscopy is based on near- or mid-infrared induced vibrational modes within a material.[25] FTIR has different modes, including transmittance, reflectance and ATR mode.[26] For the in situ FTIR transmittance mode, the incident IR beam has to pass through the electrolyte solution, which will inevitably lead to a strong absorption of the electrolyte and decrease the signal-to-noise ratio (S/N). In order to overcome the abovementioned obstacle, in situ FTIR reflectance modes are mainly used. Two main approaches toward in situ FTIR spectroscopy cell design, the internal and external reflection configurations (Figure 4), have been developed.[6]

3.1. SNIFTIRS

In the external reflection configuration, an electrode is closely coated onto an optical window made of the reflection materials (i.e., CaF_2) and a few micrometers of electrolyte solution separates the electrolyte and the optical window, which ensures a short path length through the liquid and a maximum IR illumination of the electrode. By measuring a reference spectrum at a potential where no reaction takes place, and measuring a sample spectrum, a ratio of the two spectra is obtained. Under the experiment conditions, the IR mode is also called SNIFTIRS,[27] which is mainly applied for interface research. Based on the abovementioned structural design, the choice of electrode materials is diverse, including metal single crystal electrodes, nanomaterial electrodes, oxide material electrodes and carbon material electrodes. SNIFTIRS can determine both adsorbates and solution species involved in electrochemical reactions simultaneously.

The stability of electrolyte solution is the most important factor affecting the performance of Li–O_2 batteries, and is

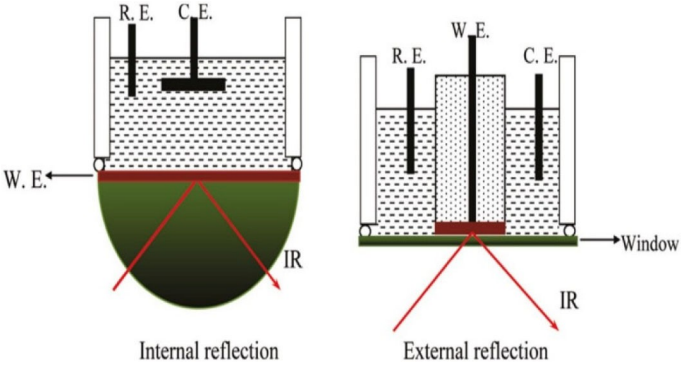

Figure 4. Schematic presentations of in situ FTIRS cell with internal and external reflection configurations. Reproduced from Ref. [6] with permission. Copyright (2016) Elsevier.

closely related to the cycle life. Calvo and co-workers[28] employed the IR method to systematically investigate the stability of DMSO-based electrolytes for Li–O_2 batteries. First, ex situ IR transmission spectra were applied to measure the stability of DMSO in the presence of O_2^- and Li_2O_2. As shown in Figure 5a, in a short time (24 h), no obvious changes in the IR spectra of DMSO were obtained both in the presence of O_2^- and Li_2O_2, indicating that DMSO is stable in the above two oxygen species with a short time. However, on long time scales (a 2 months period), new peaks at 1335, 1293, and 1142 cm^{-1} occurred in the presence of O_2^-, that corresponded to the characteristic peak of dimethyl sulfone ($DMSO_2$). The result showed that DMSO is unstable and decomposes into $DMSO_2$ in the presence of O_2^- after a 2 months period. Using the ex situ IR method makes it difficult to estimate the real electrochemical environment of the Li–O_2 batteries because the lifetime of O_2^- is very short in the presence of Li^+. To overcome this issue, the SNIFTIRS mode was performed with the CaF_2 window in the article. Under different experimental conditions (different salt cations or gas atmospheres), the adsorbed species on the electrode surface and interface in a DMSO electrolyte system were investigated (Figure 5b–5d). First of all, with the Au working electrode, the same phenomenon occurred under different experimental conditions. Namely, the formation peaks (1142 and 1295 cm^{-1}) of $DMSO_2$ and the consumption peak (3500 cm^{-1}) of H_2O were detected when the potential was higher than 4.2 V, and the intensity of these peaks increased with an increase in the anodic potential. According to the results of IR experiments, the authors proved that the decomposition of DMSO to form $DMSO_2$ at high potentials (4.2 V) was not a result of the present of oxygen species in the solvents, but rather the traces of water. Subsequently, they further explored the influence of different catalysts on the stability of DMSO electrolytes. Compared with the Au working electrode, the decomposition voltage of DMSO electrolytes was advanced to 3.5 V when Pt was used as a catalyst. Combined with several other in situ methods, including electrochemical quartz crystal microbalance (EQCM), differential electrochemical mass spectrometry (DEMS) and XPS, they provided a deeper insight into the decomposition of DMSO in Li–O_2 batteries.[29] Namely, Li_2O_2 reacts with DMSO solvent during the cell operation. As a result, Li_2CO_3 by-product is produced and CO_2 gas is released at a high potential of 4.5 V.

In addition, Llave and co-workers[30] systematically investigated the electrochemical stability of glyme-based electrolytes using SNIFTIRS experiments. This article brings several main insights. First, according to the formation peak (~ 2300 cm^{-1}) of CO_2, the authors confirmed that tetraglyme (TEGDME) is intrinsically unstable and its degradation occurs at 3.6 V in the presence and absence of O_2. The presence of O_2 will promote the decomposition of the solvent. Second, the effects of the chemical nature of the salt in the TEGDME electrolyte system were measured by evaluating the area of the CO_2 peak. They discovered that a higher free lithium ion concentration in the TEGDME electrolyte led to a larger CO_2 peak area, indicating that the solvent decomposed more easily. The reason is that more free Li^+ will have a stronger interaction

© 2021 Wiley-VCH GmbH

25666223, 2021, 6, Downloaded from https://chemistry-europe.onlinelibrary.wiley.com/doi/10.1002/batt.202000283 by University of Ulsan, Wiley Online Library on [11/11/2025]. See the Terms and Conditions (https://onlinelibrary.wiley.com/terms-and-conditions) on Wiley Online Library for rules of use; OA articles are governed by the applicable Creative Commons License

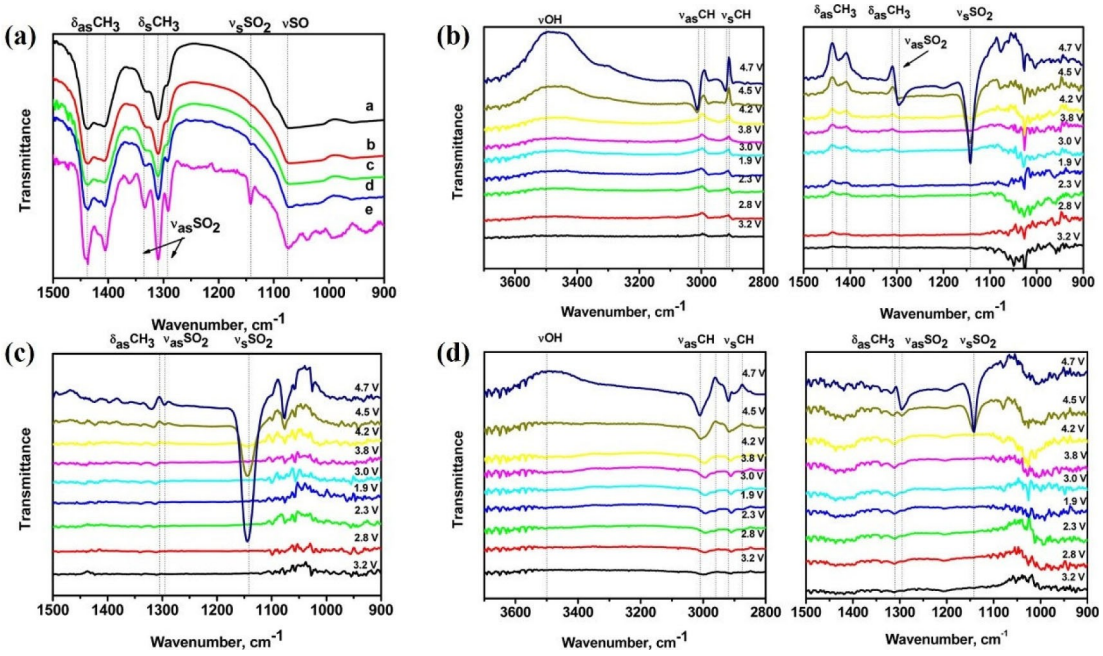

Figure 5. a) ex-situ FTIR spectra of solutions: a: pure DMSO; b: DMSO with Li_2O_2, measured 24 h after preparation; c: DMSO with KO_2, measured 24 h after preparation; d: DMSO with Li_2O_2, measured 2 months after preparation; e: DMSO with KO_2, measured 2 months after preparation. b–d) In situ IR spectra taken in a solution of DMSO on an Au working electrode. b) 0.1 M $LiPF_6$, saturated in O_2; c) 0.1 M $TBAPF_6$, deoxygenated condition; d) 0.1 M $TBAPF_6$, saturated in O_2. Reproduced from Ref. [28] with permission. Copyright (2013) American Chemical Society.

with TEGDME, resulting in the polarization and consequent destabilization of the solvent. When the cathodic salt was TBA^+, the solvent was decomposed to a high degree under a lower potential (~3 V). Finally, they further investigated the stability of diglyme (DG) solvent and the effect of water content. Compared with TEGDME electrolyte, DG showed better stability in Li–O_2 batteries. In the presence of water, the solvent decomposition was exacerbated and the decomposition onset potential advanced in an DG-based electrolyte system, which was probably related to singlet oxygen generation. Similarly, the SNIFTIRS technique was also applied to investigate the stability of ionic liquid in Li–O_2 batteries.[31]

SNIFTIRS provides us with information about the adsorption species on the interface of working electrodes. However, the IR signal is still weakened due to the inevitable adsorption of the electrolyte when the IR beam crosses a thin solution layer.[26a] In addition, the mass transportation may be seriously restricted in thin layer configuration between the thin layer and the bulk solution.[6] In order to further improve the S/N, the ATR mode is adopted.

3.2. ATR Mode

In the internal reflection configuration, the ATR mode is usually employed for in situ FTIR spectroscopy. In the ATR mode, a thin metal film deposited on an IR transparent prism with a high refractive index is used as the working electrode.[32] The high refractive index materials are mainly ZnSe, ZnS, Si and Ge. The IR beam is directed so as to enter into the light prism and is totally reflected before it leaves the crystal. Because the IR beam does not pass through the electrolyte solution, a thick solution layer can be used and the sensitivity of ATR mode is high. In addition, some thin metal films (such as Au, Pt, Pd, etc.) deposited on the IR transparent prism can achieve surface enhancement signals in the interface region, which will further improve the sensitivity of the ATR technique.[33] ATR mode has been widely applied for studying electrocatalytic reactions and processes.[34] While, the application of the ATR mode in nonaqueous Li–O_2 batteries has been reported a few times. A challenge of using the ATR mode in metal–O_2 batteries is the restricted spectral range of typical refractive index materials. For example, because of the inherent characteristics of a silicon prism, its IR spectroscopic window is 1200–4000 cm^{-1}, which limits its application in detecting ORR products (below 1200 cm^{-1}). In order to obtain the information of superoxides and some metal peroxides, a ZnSe prism (low frequency can be as low as 550 cm^{-1}) can be used as the primary reflection element.

Hardwick and co-workers[35] first applied the ATR-SEIRAS technique for the Li–O_2 batteries system. The degradation pathways of propylene carbonate (PC) in Li–O_2 batteries were researched with an Au thin film electrode and a ZnSe prism. The SEIRA spectra (Figure 6) obtained at various applied potentials demonstrated that the cationic species of salt in the electrolyte play an important role in the degradation of PC solvent. Within a tetraethylammonium perchlorate ($TEAClO_4$) salt electrolyte system, no obvious decompositions of PC solvent were detected in an oxygenated or deoxygenated environment (Figure 6c). When the cationic species was an alkali metal cation (i.e., Li^+), the PC solvent underwent a ring-opened reaction in an oxygen atmosphere and formed a ring-

© 2021 Wiley-VCH GmbH

25666223, 2021, 6, Downloaded from https://chemistry-europe.onlinelibrary.wiley.com/doi/10.1002/batt.202000283 by University of Ulsan, Wiley Online Library on [11/11/2025]. See the Terms and Conditions (https://onlinelibrary.wiley.com/terms-and-conditions) on Wiley Online Library for rules of use; OA articles are governed by the applicable Creative Commons License

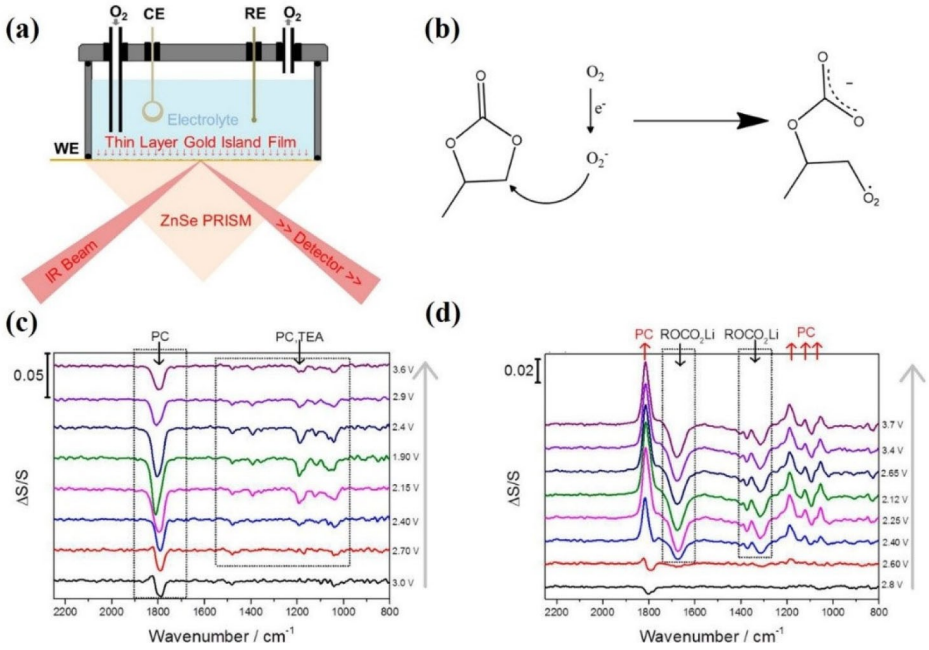

Figure 6. a) Schematic of SEIRA spectroelectrochemical cell; b) Superoxide Induced Ring opening in PC; c–d) SEIRA spectra recorded for an Au thin film electrode in oxygen saturated different electrolyte at various representative electrode potentials. c) 0.1 M $TEAClO_4$/PC and d) 0.1 M $LiClO_4$/PC. Reproduced from Ref. [35] with permission. Copyright (2016) American Chemical Society.

opened carbonate species, $ROCO_2Li$ (Figure 6b and 6d), which was consistent with the previous reports.[36] This was mainly due to the coordination of Li^+ to the carbonyl group, which promotes the degradation of PC solvent by superoxides. Because of the steric hindrance of bulky TEA^+, it cannot coordinate to the carbonyl group of the PC solvent, and the degradation of ethereal carbon by superoxides is undesirable. The same electrolyte system was studied by Ye et al. using several spectroscopy methods (SFG, SERS and UV-vis absorption spectroscopy) simultaneously.[3f] Their results showed that the PC solvent was unstable, and O_2^- induced a ring-opening reaction both in Li^+-free and Li^+-containing electrolyte systems. The variation in findings of the two articles may be due to the different selectivities and sensitivities of those measurements. Therefore, it is essential to combine different measurements to obtain reliable information. However, it is important to note that while the system does not account for a real electrode/electrolyte interface, it does give us a direct insight to understand the reaction pathway and an important analytical approach for filtering promising electrolytes in Li–O_2 batteries is established.

In situ FTIR can also be used to characterize oxygen reduction intermediates or products. Hardwick's group[37] further investigated the oxygen reduction products in non-aqueous metal–oxygen (Li–O_2 and Na–O_2) batteries using the ATR-SEIRAS technique. Combined with the coupled-cluster method including perturbative triple excitations [CCSD(T)] calculations, the influence of electrolyte composition on the IR activity of these oxygen reduction species was confirmed. As shown in Figure 7, the alkali metal superoxides (LiO_2 and NaO_2, ν_{O-O} 1125 cm^{-1}) and Li_2O_2 (ν_{Li-O} 826 cm^{-1}) were IR active in the

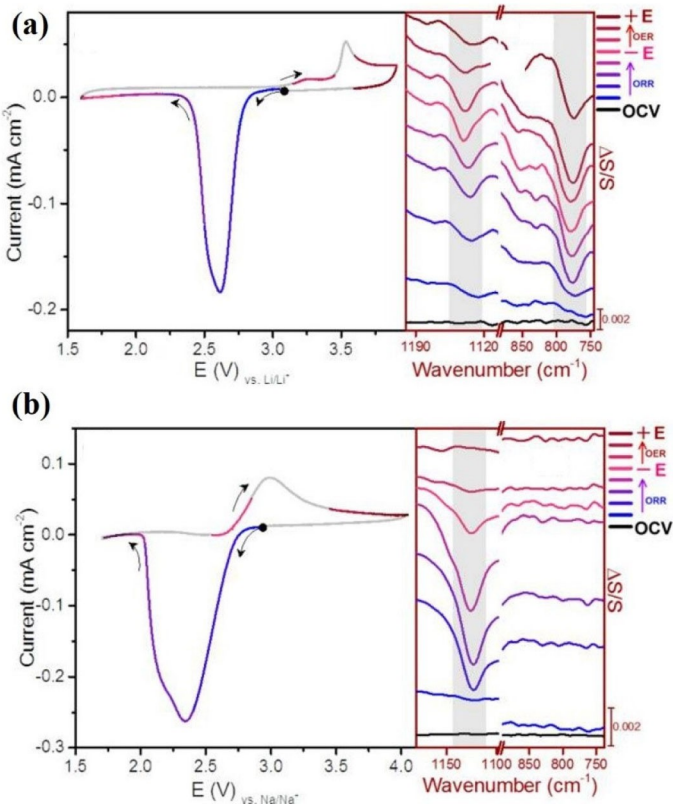

Figure 7. CV of ORR/OER at 10 mV/s scan rate in O_2 purged DMSO electrolyte solution on a Au electrode and corresponding in situ SEIRA spectra. a) 0.1 M LiOTf and b) 0.1 M NaOTf. Reproduced from Ref. [37] with permission. Copyright (2017) American Chemical Society.

© 2021 Wiley-VCH GmbH

25666223, 2021, 6, Downloaded from https://chemistry-europe.onlinelibrary.wiley.com/doi/10.1002/batt.202000283 by University of Ulsan, Wiley Online Library on [11/11/2025]. See the Terms and Conditions (https://onlinelibrary.wiley.com/terms-and-conditions) on Wiley Online Library for rules of use; OA articles are governed by the applicable Creative Commons License

25666223, 2021, 6, Downloaded from https://chemistry-europe.onlinelibrary.wiley.com/doi/10.1002/batt.202000283 by University of Ulsan, Wiley Online Library on [11/11/2025]. See the Terms and Conditions (https://onlinelibrary.wiley.com/terms-and-conditions) on Wiley Online Library for rules of use; OA articles are governed by the applicable Creative Commons License

electrolytes composed of DMSO with a Li^+ or Na^+ salt. No obvious IR peaks of oxygen reduction species were detected in acetonitrile (MeCN)-based electrolytes with a Li^+ or Na^+ salt. Meanwhile, when TEA^+ salt was added into the aforementioned MeCN-based electrolytes, the IR peaks of LiO_2 and NaO_2 were observed. This was mainly due to the solvation of oxygen reduction species, which is critical to the IR activity of these species. DMSO solvent and TEA^+ salt have a strong solvation with those oxygen reduction species, leading to the IR activity of these species. Through the above ATR-SEIRAS studies, they confirmed that the high donor number solvent DMSO (29.8 kcal mol^{-1}) promotes a solvent-mediated reaction routes during discharge process owing to strong solvation, and the low donor number solvent MeCN (14.1 kcal mol^{-1}) promotes a surface-confined reaction route owing to weak solvation. Similar to Raman spectroscopy, the IR activity of metal superoxides also depends strongly on their environment. The superoxides and peroxides have no IR activity of the O–O bond without metal ions because of their innate homopolar nature. Molecular metal superoxides and peroxides have IR activities[38] and that can be detected within electrolytes containing a high donor number solvent (such as DMSO) or TEA^+. However, these IR bands cannot be detected within electrolytes containing a low donor number solvent (MeCN) because the metal superoxides and peroxides with the film-like morphologies have no IR activity.[38] The advantage of the SEIRAS technique is that the reaction pathways between solution-mediated and surface-reaction mechanisms can be distinguished.

In addition, Wang's group[39] unequivocally identified the oxygen reduction intermediate with different kinds of modified redox electrolytes through ATR model FTIR measurement. In a duroquinone (DQ)-based electrolyte, an ORR intermediate (DQ–Li–O_2^- complex) was unambiguously validated, while no similar ORR intermediates were detected in either ethyl viologen (EV) electrolyte or the dual redox mediators with DQ and EV. That was due to the low affinity of the EV solvent towards the reduced oxygen species, which eliminated the soluble DQ–Li–O_2^- complex. Using the in situ FTIR method, they concluded that, with the dual redox mediators (DQ and EV) electrolyte system, the ORR process could be regulated by suppressing the formation of soluble superoxide species while maintaining good reaction kinetics.

4. Summary and Outlook

This paper reviews some recent developments and applications of in situ Raman spectroscopy and in situ FTIR spectroscopy for Li–O_2 batteries. The SERS technique and FTIR spectroscopy have been shown to offer great advantages for probing the structures of reaction intermediates, products and solvents on the electrode surface because of the intrinsic surface selectivity, which provide rich information on the electrode/electrolyte interface. The SERS technique mainly identifies the superoxide and peroxide species, which are Raman-active, and the understanding of the reaction mechanisms under different conditions for Li–O_2 batteries has been discussed. For the FTIR technique, two in situ FTIR (SNIFTIRS and ATR-SEIRAS) methods are introduced for use in Li–O_2 batteries. The stabilities of the different electrolytes, the factors influencing the IR activity of these oxygen reduction species, as well as the oxygen reduction intermediate species have been systematically summarized by in situ FTIR techniques, which further helps us understand the reaction mechanism and the failure mechanism of the cell. The two vibrational spectroscopic methods are complementary tools to investigate the reaction mechanisms of the cell and the stability of solvents in Li–O_2 batteries. However, not all vibrational modes of intermediates and solvents are Raman-active or IR-active. Furthermore, the application of thin metal films in the two vibrational spectroscopic methods is still very limited. The biggest challenge of interface research is that the interface of Li–O_2 batteries is complex, constantly changing and irreversible. Therefore, to obtain reliable experimental results, other technologies, such as SFG spectroscopy, UV-vis absorption spectroscopy, EQCM, DEMS, XPS and the theoretical calculation methods, also need to be considered comprehensively. Through such collaborative efforts, we hope that in situ Raman and in situ FTIR studies will also push forward the understanding and development of Li–O_2 batteries as well as other battery systems.

Acknowledgements

The authors acknowledge funding support from Shanghai Science and Technology Committee (19DZ2270100), and the Science and Technology Commission of Shanghai Municipality (19ZR1403600 & 19DZ2270100), China.

Conflict of Interest

The authors declare no conflict of interest.

Keywords: FTIR spectroscopy · in situ techniques · Li–O_2 batteries · Raman spectroscopy · reaction mechanism

[1] a) W. Zhao, X. Mu, P. He, H. Zhou, *Batteries Supercaps* **2019**, *2*, 803–819; b) Z. Peng, S. A. Freunberger, Y. Chen, P. G. Bruce, *Science* **2012**, *337*, 563–566; c) P. Zhang, Y. Zhao, X. B. Zhang, *Chem. Soc. Rev.* **2018**, *47*, 2921–3004.
[2] Z. Lyu, Y. Zhou, W. Dai, X. Cui, M. Lai, L. Wang, F. Huo, W. Huang, Z. Hu, W. Chen, *Chem. Soc. Rev.* **2017**, *46*, 6046–6072.
[3] a) Y. C. Lu, E. J. Crumlin, T. J. Carney, L. Baggetto, S. H. Yang, *J. Phys. Chem. C* **2013**, *117*, 25948–25954; b) F. S. Gittleson, K. P. C. Yao, D. G. Kwabi, S. Y. Sayed, W. H. Ryu, Y. Shao-Horn, A. D. Taylor, *ChemElectroChem* **2015**, *2*, 1446–1457; c) A. J. Cowan, L. J. Hardwick, *Annu. Rev. Anal. Chem.* **2019**, *12*, 323–346; d) S. Ganapathy, B. D. Adams, G. Stenou, M. S. Anastasaki, K. Goubitz, X. F. Miao, L. F. Nazar, M. Wagemaker, *J. Am. Chem. Soc.* **2014**, *136*, 16335–16344; e) A. Ge, D. Zhou, K.-i. Inoue, Y. Chen, S. Ye, *J. Phys. Chem. C* **2020**, *124*, 17538–17547; f) Q. Peng, Y. Qiao, K. Kannari, A. Ge, K.-i. Inoue, S. Ye, *J. Phys. Chem. C* **2020**, *124*, 15781–15792; g) A. Ge, K.-i. Inoue, S. Ye, *J. Chem. Phys.* **2020**, *153*, 170902.
[4] C. V. Raman, K. S. Krishnan, *Nature* **1928**, *121*, 501–502.
[5] a) Q. Yu, S. Ye, *J. Phys. Chem. C* **2015**, *119*, 12236–12250; b) D. Zhai, K. C. Lau, H. H. Wang, J. Wen, K. Amine, *Nano Lett.* **2015**, *15*, 1041–1046.

© 2021 Wiley-VCH GmbH

[6] J. Y. Ye, Y. X. Jiang, T. Sheng, S. G. Sun, *Nano Energy* **2016**, *29*, 414–427.
[7] a) J. Hu, Y. Li, Y. Zhen, M. Chen, H. Wan, *Chinese J. Catal.* **2021**, *42*, 367–375; b) L. Chen, T. Zhu, R. Ning, *J. Hazard. Mater.* **2019**, *363*, 90–98; c) S. Zhu, B. Jiang, W. B. Cai, M. Shao, *J. Am. Chem. Soc.* **2017**, *139*, 15654–15667.
[8] Z. Q. Tian, B. Ren, D. Y. Wu, *J. Phys. Chem. B* **2002**, *106*, 9463–9483.
[9] D. J. Gardiner, P. R. Graves, *Practical Raman Spectroscopy*, Springer-Verlag, **1989**.
[10] a) J. P. Camden, J. A. Dieringer, J. Zhao, R. P. Van Duyne, *Acc. Chem. Res.* **2008**, *41*, 1653–1661; b) A. B. Zrimsek, N. Chiang, M. Mattei, S. Zaleski, R. P. V. Duyne, *Chem. Rev.* **2017**, *117*, 7583–7613.
[11] X. B. Han, K. Kannari, S. Ye, *Curr. Opin. Electrochem.* **2019**, *17*, 174–183.
[12] Z. Q. Peng, S. A. Freunberger, L. J. Hardwick, Y. H. Chen, V. Giordani, F. Bardé, P. Novák, D. Graham, J.-M. Tarascon, P. G. Bruce, *Angew. Chem. Int. Ed.* **2011**, *123*, 6351–6355.
[13] a) L. Johnson, C. Li, Z. Liu, Y. Chen, S. A. Freunberger, P. C. Ashok, B. B. Praveen, K. Dholakia, J. M. Tarascon, P. G. Bruce, *Nat. Chem.* **2014**, *6*, 1091–1099; b) P. M. Radjenovic, L. J. Hardwick, *Phys. Chem. Chem. Phys.* **2019**, *21*, 1552–1563; c) P. M. Radjenovic, L. J. Hardwick, *Faraday Discuss.* **2018**, *206*, 379–392.
[14] F. S. Gittleson, W. H. Ryu, A. D. Taylor, *ACS Appl. Mater.* **2014**, *6*, 19017–19025.
[15] D. Aurbach, B. D. Mccloskey, L. F. Nazar, P. G. Bruce, *Nat. Energy* **2016**, *16128*.
[16] X. Zhang, L. Guo, L. Gan, Y. Zhang, Z. Peng, *J. Phys. Chem. Lett.* **2017**, *8*, 2334–2338.
[17] a) Q. Lin, Z. H. Cui, J. Y. Sun, H. Y. Huo, C. Chen, X. X. Guo, *ACS Appl. Mater. Interfaces* **2018**, *10*, 18754–18760; b) B. D. Adams, C. Radtke, R. Black, M. L. Trudeau, K. Zaghib, L. F. Nazar, *Energy Environ. Sci.* **2013**, *6*, 1772–1778.
[18] F. S. Gittleson, K. P. C. Yao, D. G. Kwabi, S. Y. Sayed, W.-H. Ryu, Y. Shao-Horn, A. D. Taylor, *ChemElectroChem* **2015**, *2*, 1446–1457.
[19] E. S. Rittner, *J. Chem. Phys.* **1951**, *19*, 1030–1035.
[20] L. Andrews, R. R. Smardzewski, *J. Chem. Phys.* **1973**, *58*, 2258–2261.
[21] X. Ren, Y. Wu, *J. Am. Chem. Soc.* **2013**, *135*, 2923–2926.
[22] J. T. Frith, A. E. Russell, N. Garcia-Araez, J. R. Owen, *Electrochem. Commun.* **2014**, *46*, 33–35.
[23] C. Li, O. Fontaine, S. A. Freunberger, L. Johnson, S. Grugeon, S. Laruelle, P. G. Bruce, M. Armand, *J. Phys. Chem. C* **2014**, *118*, 3393–3401.
[24] T. A. Galloway, L. J. Hardwick, *J. Phys. Chem. Lett.* **2016**, *7*, 2119–2124.
[25] S. Kumar, T. Verma, R. Mukherjee, F. Ariese, S. Umapathy, *Chem. Soc. Rev.* **2016**, *47*, 1879–1900.
[26] a) S. F. Amalraj, D. Aurbach, *J. Solid State Electrochem.* **2011**, *15*, 877–890; b) Y. Deng, S. Dong, Z. Li, H. Jiang, X. Zhang, X. Ji, *Small Methods* **2018**, *1700332*.
[27] Q. Yuan, H. A. Doan, L. C. Grabow, S. R. Brankovic, *J. Am. Chem. Soc.* **2017**, *139*, 13676–13679.
[28] N. Mozhzhukhina, L. P. Méndez De Leo, E. J. Calvo, *J. Phys. Chem. C* **2013**, *117*, 18375–18380.
[29] N. Mozhzhukhina, F. Marchini, W. R. Torres, A. Y. Tesio, L. P. M. D. Leo, F. J. Williams, E. J. Calvo, *Electrochem. Commun.* **2017**, *80*, 16–19.
[30] G. Horwitz, E. J. Calvo, L. P. M. D. Leo, E. d. l. Llave, *Phys. Chem. Chem. Phys.* **2020**, *22*, 16615–16623.
[31] N. Mozhzhukhina, A. Y. Tesio, L. P. M. D. Leo, E. J. Calvo, *J. Electrochem. Soc.* **2017**, *164*, A518–A523.
[32] D. R. Macfarlane, M. Forsyth, P. C. Howlett, M. Kar, J. Zhang, *Nat. Rev. Mater.* **2016**, *1*, 15005.
[33] A. Hartstein, J. R. Kirtley, J. C. Tsang, *Phys. Rev. Lett.* **1980**, *45*, 201–204.
[34] a) N. Simantini, M. P. I. James, V. K. Alison, *Angew. Chem.* **2018**, *130*, 1–5; *Angew. Chem. Int. Ed.* **2018**, *57*, 1–1; b) M. Dunwell, X. Yang, Y. Yan, B. Xu, *J. Phys. Chem. C* **2018**, *122*, 24658–24664; c) R. Jamwal, Amit, S. Kumari, B. Balan, D. K. Singh, *Spectrochim. Acta Part A Mol. Biomol. Spectrosc.* **2020**, *244*, 1386–1425; d) S. Zhu, T. Li, W. B. Cai, M. Shao, *ACS Energy Lett.* **2019**, *4*, 682–689; e) H. Wang, Y. W. Zhou, W. B. Cai, *Curr. Opin. Electrochem.* **2017**, *1*, 73–79.
[35] J. P. Vivek, N. Berry, G. Papageorgiou, R. J. Nichols, L. J. Hardwick, *J. Am. Chem. Soc.* **2016**, *138*, 3745–3751.
[36] S. A. Freunberger, Y. Chen, Z. Peng, J. M. Griffin, L. J. Hardwick, F. Bardé, P. Novák, P. G. Bruce, *J. Am. Chem. Soc.* **2011**, *133*, 8040–8047.
[37] J. P. Vivek, N. G. Berry, J. L. Zou, R. J. Nichols, L. J. Hardwick, *J. Phys. Chem. C* **2017**, *121*, 19657–19667.
[38] S. A. Freunberger, Y. Chen, Z. Peng, J. M. Griffin, L. J. Hardwick, F. Barde, P. Novak, P. G. Bruce, *J. Am. Chem. Soc.* **2011**, *133*, 8040–8047.
[39] Y. G. Zhu, F. W. T. Goh, R. Yan, S. Wu, S. Adams, Q. Wang, *Phys. Chem. Chem. Phys.* **2018**, *20*, 27930–27936.

Manuscript received: November 19, 2020
Revised manuscript received: February 7, 2021
Accepted manuscript online: February 10, 2021
Version of record online: February 18, 2021

© 2021 Wiley-VCH GmbH

25666223, 2021, 6, Downloaded from https://chemistry-europe.onlinelibrary.wiley.com/doi/10.1002/batt.202000283 by University of Ulsan, Wiley Online Library on [11/11/2025]. See the Terms and Conditions (https://onlinelibrary.wiley.com/terms-and-conditions) on Wiley Online Library for rules of use; OA articles are governed by the applicable Creative Commons License